RSC Advances

PAPER

Cite this: *RSC Adv.*, 2021, **11**, 18288

Effect of H_2SiF_6 modification of IM-5 on catalytic performance in benzene alkylation with ethylene†

Yunping Zhai, Junwen Chen, Yongrui Wang,* Yibin Luo and Xingtian Shu

Ethylbenzene (EB) is an important bulk chemical intermediate. The vapor-phase process is considered to be more efficient than the liquid-phase process when using dilute ethylene (*e.g.* FCC or DCC off-gas) as the feed due to its high ethylene space velocity. However, realizing a balance between reducing the xylene formation and enhancing the EB selectivity is still a challenge due to the poor performance of ZSM-5 at low reaction temperature. This study concerns an IM-5 zeolite (IMF topology) modified by H_2SiF_6, with 89% ethylbenzene selectivity, 98.6% total EB + DEB selectivity and only 540 ppm of xylene at 330 °C. IM-5 zeolites with different Si/Al_2 ratios (40–170) were prepared by H_2SiF_6 modification and their catalytic performance in vapor phase alkylation of benzene with ethylene was investigated. There was an obvious decrease in the acid sites and acid strength of IM-5 in the H_2SiF_6 treatment process, which led to a slight decrease in ethylbenzene selectivity and a significant decline in xylene yield. Under the conditions of complete ethylene conversion, the selectivity to EB + DEB increased from 96.1% to 98.6% in the parent I-40 and modified IM-5. Compared with ZSM-5 that has a similar acidity, the slightly bigger channel opening makes IM-5 more conductive to the formation and diffusion of DEB while xylene may present adverse effects. The 120 hour-lifetime test showed that IM-5 (I-110) has superior activity, equivalent stability, higher DEB selectivity and a much lower xylene selectivity in comparison with ZSM-5. The catalytic performance of the IM-5 zeolite in the vapor phase process provides a new choice for the production of ethylbenzene.

Received 27th March 2021
Accepted 10th May 2021

DOI: 10.1039/d1ra02427b

rsc.li/rsc-advances

1. Introduction

As one of the most important intermediates in the petrochemical industry, ethylbenzene (EB) is mainly used to produce styrene.[1–3] Ethylbenzene is mainly produced by the alkylation of benzene with ethylene. The process was mainly catalyzed by the corrosive Friedel–Crafts catalyst (mainly referring to $AlCl_3$–HCl) in the past. However, zeolite-based catalysts are now commonly applied, including ZSM-5 (for vapor-phase alkylation), beta (for-liquid-phase alkylation) and MCM-22 (for liquid phase alkylation).[3]

Compared to the liquid-phase process, the ZSM-5 catalyzed vapor-phase process has better flexibility in the selection of ethylene resources, including the dilute ethylene from FCC, DCC and ethane cracking units in refineries.[4,5] Moreover, the medium pore ZSM-5-based catalysts have been proven to suppress the formation of bulkier products due to steric hindrance, resulting in better EB selectivity and catalyst stability.[5,6] However, the two types of 10-member ring channel systems (0.51 nm × 0.55 nm and 0.53 nm × 0.56 nm) in the ZSM-5 structure exhibits stronger resistance for the pore diffusion process, limiting the mass transport to and from the acid sites.[7] Thus, a relatively higher reaction temperature (*e.g.* 360–420 °C) is usually adopted in the vapor-phase process.[8] Under the given temperature, more xylenes, residues and other undesired by-products are generated through side reactions, such as cracking, isomerization or disproportionation.[9] It is believed that most part of xylene is generated by the side reactions, *e.g.* EB isomerization, on the strong acid sites of catalysts. Furthermore, the formation of xylene can also be accelerated when raising the reaction temperature.[10] Xylene is one of the most important by-products and their boiling points are very close to that of ethylbenzene. There are no economic ways to separate xylene from ethylbenzene.[11] As a result, the purity of EB is affected. Therefore, reducing the reaction temperature and decreasing the strength of zeolite acid sites are both effective ways to enhance the selectivity in benzene alkylation with ethylene. However, it is difficult for ZSM-5 to realize the goal due to its narrow 3D 10-ring pore system. The strong diffusion resistance to aromatics and quick ethylene oligomerization at a relative low reaction temperature will lead to a rapid deactivation of ZSM-5.[12,13] Therefore, developing an alternative catalyst is crucial for the synthesis of ethylbenzene. Taking into consideration of the steric hindrance and mass transport, the IM-5 (framework type: IMF) zeolite may be an ideal candidate for vapor phase alkylation of benzene with ethylene as its slightly bigger channel opening and adjustable acidity.

State Key Laboratory of Catalytic Material and Reaction Engineering, Research Institute of Petroleum Processing, Sinopec, Beijing 100083, China. E-mail: wangyr.ripp@sinopec.com

† Electronic supplementary information (ESI) available. See DOI: 10.1039/d1ra02427b

IM-5 was firstly synthesized by Benazzi in 1998 with 1,5-bis(*N*-methyl-pyrrolidinium) pentane as a structure-directing agent[14] and its crystal structure was resolved by an enhanced charge flipping structure-solution algorithm method in 2007.[15] In contrast to ZSM-5, which channel structure consists of intersectional straight and sinusoidal ten-membered ring channels (5.1 × 5.5 Å, 5.3 × 5.6 Å) and an intersection cavity of about 8.6 Å, IM-5 consists of two 2D channel systems. One 2D system has channel diameters of 5.5 × 5.6 Å and 5.3 × 5.4 Å, while the other has channel diameters of 4.8 × 5.4 Å and 5.1 × 5.3 Å. These two 2D systems are connected by a channel with a diameter of 5.3 × 5.9 Å from each other and generate a bigger cavity (10.4 Å) in the channel intersections.[16] With similar acidic properties (*e.g.* similar acid strength and Brønsted to Lewis acid site ratio),[17] a better thermal and hydrothermal stability[18,19] as well as higher adsorption capacity of alkyl aromatic hydrocarbon[20] compared to ZSM-5, IM-5 is expected to replace ZSM-5 in many petrochemical processes. The catalytic performance of IM-5 zeolite has been investigated in alkane hydro-isomerization,[21] methylation of toluene,[22,23] disproportionation of toluene[24] and alkylation of benzene with ethanol[25] as well as alkylation with methanol.[26] However, the application of IM-5 zeolite in the vapor phase alkylation of benzene with ethylene has not been reported.

The catalytic performance of the zeolites depends upon the acidity controlled by the framework Si/Al_2 ratio, which can be regulated either during synthesis or by post-treatment dealumination methods. Steam treatments, $SiCl_4$ treatment, reaction with chelating agents such as ammonium hexafluorosilicate (NH_4SiF_6), oxalic acid, *etc.* and leaching with mineral acid are some of the common post-synthesis methods used to control the acidity of the zeolites. Due to the crystallization of pure IM-5 is possible only from synthesis mixtures with a narrow range of SiO_2/Al_2O_3,[27] thus, it is an effective way to regulate the Si/Al_2 ratio of IM-5 by post-treatment method. Compared with other methods, the dealumination with hexafluorosilicic acid (H_2SiF_6) is an effective way to increase Si/Al_2 ratio while preserving the structural and textural properties of the zeolite.[28] Moreover, the effect of H_2SiF_6 treatment on the physical and chemical properties of IM-5 has not been systematically studied, even though it is of great significance for establishing the correlation between the properties of zeolites and its catalytic performance on vapor-phase alkylation of benzene with ethylene. Herein, we report an IM-5 zeolite (IMF topology) modified by H_2SiF_6, with an 89% ethylbenzene selectivity, 98.6% total EB + DEB selectivity and with only 540 ppm of xylene at 330 °C. A series of IM-5 zeolites with different Si/Al_2 ratios (40–170) were prepared by H_2SiF_6 modification and their catalytic performance in vapor phase alkylation of benzene with ethylene was explored. The structural and acidity properties of IM-5 before and after modification by H_2SiF_6 were investigated. Characterization techniques such as X-ray diffraction, X-ray fluorescence, N_2 adsorption–desorption isotherms measurement, scanning electron microscopy, magic angle spinning nuclear magnetic resonance, and pyridine-adsorption IR measurement were adopted to characterize the changes in structural and acidities for the modified materials. The results suggest that H_2SiF_6 treatment is an effective way to increase the Si/Al_2 ratio of IM-5. The ethylated benzene (EB + DEB) selectivity can be further increased and the formation of coke can be inhabited at an optimum Si/Al_2 ratio. Moreover, reducing the reaction temperature can increase the total EB + DEB selectivity and reduce xylene selectivity. The unique pore structure of IM-5 played a key role in contributing to a higher EB + DEB selectivity and a much lower xylene yield compared with ZSM-5 with a similar Si/Al_2 ratio under equivalent stability.

2. Experimental

2.1 Synthesis and preparation

IM-5 zeolite was synthesized by traditional hydrothermal synthesis as reported in the literature method.[14] The as-synthesized IM-5 zeolite was firstly calcined at 823 K for 5 h to remove the organic templates and then ion exchanged 3 times with an NH_4Cl solutions at 353 K for 3 h to obtain the parent H-IM-5 *via* subsequent calcination at 823 K for 4 h. IM-5 zeolites with different SiO_2/Al_2O_3 ratio was prepared by treating the parent H-IM-5 ($SiO_2/Al_2O_3 = 40$, denoted as I-40) with H_2SiF_6 aqueous solution at 353 K for 60 min. The concentration of H_2SiF_6 in the aqueous solution was varied from 0.05 to 0.20 mol L^{-1}. All samples were filtrated and the solids were washed with deionized water, dried at 393 K for 12 hours and calcined at 823 K for 3 h to obtain H-IM-5 samples with different SiO_2/Al_2O_3 ratio. The samples were designated as I-80, I-110, I-130 and I-170 according to their SiO_2/Al_2O_3 ratio, respectively. The H-ZSM-5 zeolite ($SiO_2/Al_2O_3 = 110$, denoted as Z-110) was obtained from the Research Institute of Petroleum Processing in order to investigate the effect of zeolite topology on product distribution in benzene alkylation with ethylene over IM-5 and ZSM-5.

2.2 Catalyst characterization

The elemental analysis of all samples were conducted with an X-ray fluorescence (XRF) spectrometer. X-ray diffraction (XRD) patterns of all samples were recorded on a Siemens D5000 diffractometer using nickel-filtered Cu Kα radiation. The relative crystallinity (R.C.) of IM-5 zeolite was calculated based on the sum of relative peak area of the reflection at 2θ range of 22.1–25.4 of the prepared sample with that of the parent IM-5 (whose R.C. was assumed as 100%). Physical adsorption/desorption of nitrogen on the samples were performed with an adsorption analyzer. The total surface area of each sample was determined with the Brunauer–Emmett–Teller (BET) method, and the micropore volume and external surface area were determined with the *t*-plot method. The mesopore size distributions profile and the mesopores volume of the samples were calculated with the Barrett–Joyner–Halenda (BJH) desorption branch of the isotherms. Chemical adsorption of NH_3 on samples were carried out with an adsorption analyzer (Autochem 2920, Micromeritics, USA). Pyridine infrared (Py-IR) spectra of the samples in the range of 1700–1300 cm^{-1} were recorded on a Fourier transform infrared FT-IR spectrometer with a resolution of 0.35 cm^{-1}. The morphologies and particle sizes of the samples were measured by using a scanning electron microscope (SEM: Quanta200F, FEI, USA) at an accelerating voltage of 20 kV. In a typical GC-MS analysis, 200 mg of the

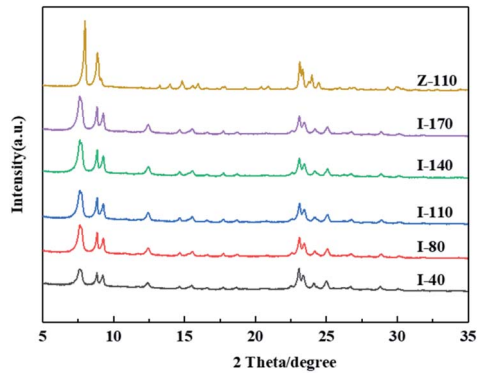

Fig. 1 XRD patterns of IM-5 and ZSM-5 samples.

used catalyst was completely dissolved in 2 mL of 40% HF solutions and neutralized with NaOH. CH_2Cl_2 (Aldrich, 99.9%) was employed to extract the organic species from the resulting solutions. The GC-MS total ion chromatograms of extracted organic phases were recorded on a Varian CP 3800 gas chromatograph equipped with a Varian 320-MSD mass-selective detector, using electron impact ionization at 70 eV.

2.3 Catalytic evaluation

The vapor-phase alkylation of benzene with ethylene was carried out in a fixed-bed reactor with an internal diameter of 12 mm. Analytical grade (99 wt%) benzene and ethylene were used. Samples were loaded and pretreated with N_2 flow at 400 °C for 2 h prior to the reaction. Benzene was firstly introduced into the reactor and then the ethylene was introduced when benzene was detected in the outlet of the condenser. The reaction temperature varied from 300 °C to 360 °C and the reaction pressure was 0.8 MPa. The ethylene weight hourly space velocity (WHSV) was 0.5 h^{-1} and the molar ratio of benzene to ethylene was 8.5 : 1. The products were analyzed by an on-line Agilent 7890A gas chromatograph, equipped with a flame ionization detector and 60 m cross-linked methyl silicone capillary column innowax (0.32 mm). The ethylene conversion and product selectivity were calculated as follows:

$$\text{Ethylene conversion } (\%) = (X_{\text{ethylene before reaction}} - X_{\text{ethylene after reaction}}) / X_{\text{ethylene before reaction}} \times 100\%$$

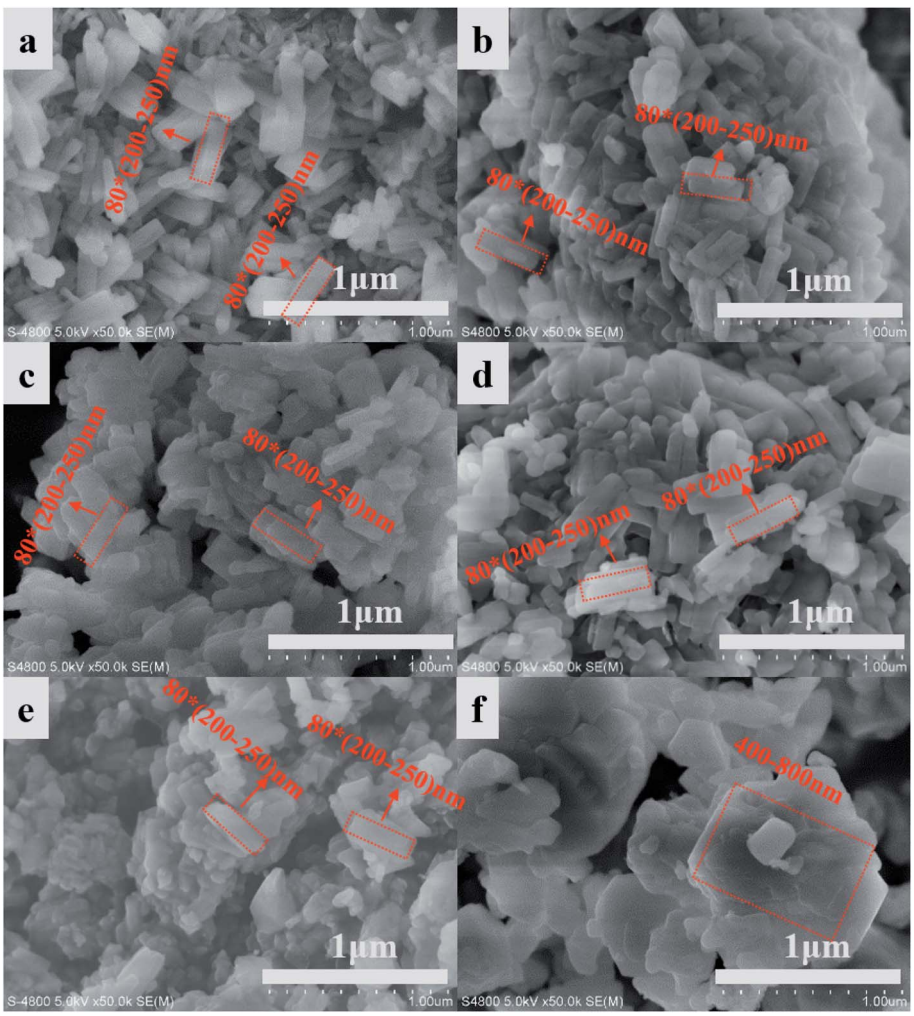

Fig. 2 SEM images and particle size distribution of IM-5 and ZSM-5: I-40 (a), I-80 (b), I-110 (c), I-140 (d), I-170 (e) and Z-110 (f).

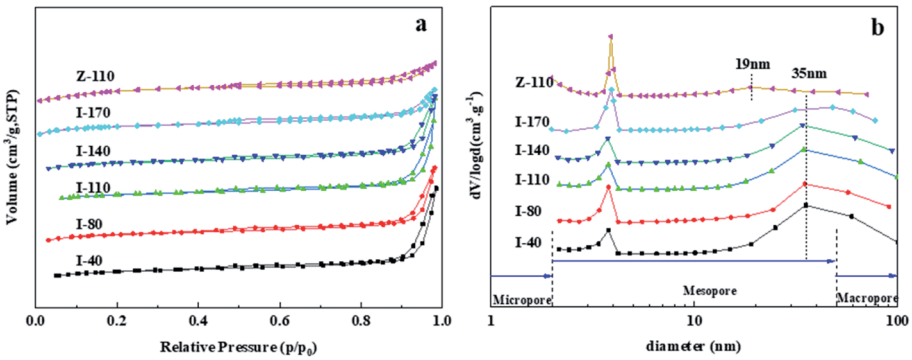

Fig. 3 N_2 adsorption–desorption isotherms (a) and BJH pore size distribution curves (b) for IM-5 and ZSM-5 samples.

$$\text{Selectivity (\%)} = (\text{amount of i\% in the products}) / \left(\sum \text{amounts of i\% in the products}\right) \times 100\%$$

where i represented one of the products, such as EB, DEB and so on.

3 Results and discussion

3.1 Textural and physicochemical characterization

The crystal structure of IM-5 zeolites and the reference ZSM-5 are shown in Fig. 1. The diffraction peaks observed in the 2θ range of 22.1–25.4 of all IM-5 samples indicate the typical IMF structure[29] without detection of any other phases. Moreover, there is no obvious decline in the crystallinity of post modified IM-5 zeolites compared with I-40, which illustrates that the structure of IM-5 was not destroyed during H_2SiF_6 treatment. In addition, ZSM-5 (Z-110) exhibits typical characteristic patterns of the MFI topology without other impurity crystal phase observed.

SEM was employed to analyse the changes of microscopic morphology of IM-5 zeolites before and after H_2SiF_6 treatment. As shown in Fig. 2, all IM-5 samples exhibit rectangular shape with crystal size of 200–250 nm in length and about 80 nm in width, which is in good agreement with that of ref. 27. In addition, all IM-5 samples have a smooth surface and dense structure, with no amorphous material found after H_2SiF_6 treatment. The results further confirm that there was no serious damage to the IM-5 structure during H_2SiF_6 treatment. The crystal size of ZSM-5 is in the range of 400–800 nm, which is incomparable to that of IM-5 zeolite. In addition, an aggregation of small crystals was observed in both IM-5 and ZSM-5 samples. Which would be further improved by the N_2 adsorption–desorption isotherms. Fig. 3(a) displays the N_2 adsorption–desorption isotherms of IM-5 and ZSM-5 samples. The corresponding data are summarized in Table 1. The curves clearly indicate that the combination characteristic of type I and type IV isotherms with a closed hysteresis loop at high relative pressure of 0.45–0.99 of both IM-5 and ZSM-5 samples. This suggest that the mesopores are mainly intergranular pores generated by the accumulation of nanosized zeolite crystals.[30–32] This is further verified in the mesopore size distributions from BJH method (Fig. 3(b)).

The mesopores are centered around 35 nm and 19 nm for IM-5 and ZSM-5, respectively. The parent I-40 sample has a large specific surface area of 343 $cm^2\ g^{-1}$ and micropore surface area of 295 $cm^2\ g^{-1}$. With the increase of SiO_2/Al_2O_3 ratio, the specific surface area, micropore surface area and micropore volume of IM-5 are all decrease, which might be associated with dealumination during the H_2SiF_6 treatment process. However, the mesopore volume of IM-5 firstly increase and then decrease with increasing SiO_2/Al_2O_3 ratio. I-110 has the largest mesopore volume of 0.271 $cm^3\ g^{-1}$. Z-110 has a specific surface area of 370 $cm^2\ g^{-1}$ and micropore volume of 0.158 $cm^3\ g^{-1}$, larger than 264 $cm^2\ g^{-1}$ and 0.121 $cm^3\ g^{-1}$ of I-110. However, the mesopore volume of Z-110 is only about 0.08 $cm^3\ g^{-1}$. The hierarchical factor (HF), defined as $(V_{Micro}/V_{total}) \times (S_{meso}/S_{BET})$, which is one of the very important factor in describing structural properties of zeolites, was calculated for the tested samples (Table 1). The HF (×100) values increased with Si/Al_2 ratio increasing from 80 to 140. Further increasing Si/Al_2 ratio to 170, the HF began to decrease.

Table 1 Textural properties and chemical composition of IM-5 and ZSM-5 samples

Samples	$C(H_2SiF_6)$ mol L^{-1}	R.C.[a] (%)	Si/Al_2[b]	HF[c] (×100)	Textural properties					
					S_{total} ($m^2\ g^{-1}$)	S_{micro} ($m^2\ g^{-1}$)	S_{ext} ($m^2\ g^{-1}$)	V_{total} ($cm^3\ g^{-1}$)	V_{micro} ($cm^3\ g^{-1}$)	V_{meso} ($cm^3\ g^{-1}$)
I-40	0	100	40	5.06	343	295	48	0.373	0.135	0.238
I-80	0.05	99.8	84	4.33	317	277	40	0.379	0.130	0.249
I-110	0.10	99.6	110	4.83	313	264	49	0.392	0.121	0.271
I-140	0.15	99.4	132	6.89	316	259	57	0.309	0.118	0.191
I-170	0.20	98.2	170	5.50	264	223	41	0.291	0.103	0.188
Z-110			110	5.20	370	341	29	0.238	0.158	0.080

[a] Relative crystallinity. [b] Si/Al_2: molar ratio detected by XRF. [c] HF: hierarchical factor, defined as $(V_{micro}/V_{total}) \times (S_{meso}/S_{BET})$.

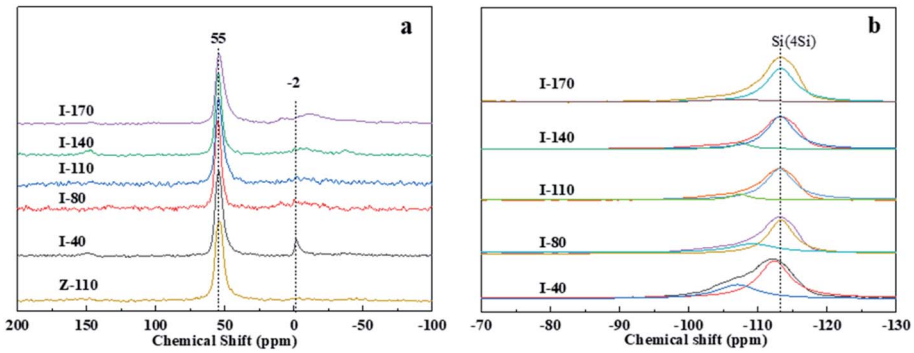

Fig. 4 ^{27}Al (a) and ^{29}Si (b) MAS NMR spectra of IM-5 and ZSM-5 samples.

Fig. 4(a) shows the ^{27}Al MAS NMR spectra of IM-5 samples before and after H_2SiF_6 treatment and ZSM-5 sample. Two types of Al coordinate centered at around 55 ppm and −2 ppm are observed in the I-40, for which tetrahedral-coordinated framework Al and octahedral-coordinated extra-framework Al are assigned respectively.[27] The extra-framework Al of IM-5 samples after the H_2SiF_6 treatment disappeared, indicating that the extra-framework Al of I-40 was removed out and no additional extra-framework Al was formed during acid treatment. The dealumination of parent IM-5 can be further confirmed by the information obtained from the ^{29}Si MAS NMR spectra. As shown in Fig. 4(b), the two signals at about −107 and −113 ppm are assigned Si (3Si, 1Al) and Si (4Si, 0Al) respectively. After the H_2SiF_6 treatment, the positions of peaks in the spectra of all IM-5 samples are not change, but the intensity of the Si (3Si, 1Al) signal is remarkably reduced with the increases of H_2SiF_6 concentration. The results indicate that the dealumination first occurred in the Si (3Si, 1Al) opposition.

The SiO_2/Al_2O_3 ratios of the parent and post modified IM-5 samples are listed in Table 1. Clearly, the SiO_2/Al_2O_3 of IM-5 samples increased greatly with the increase of H_2SiF_6 concentration. There are no distinct differences in the NH_3-TPD curves between I-110 and Z-110, indicating that the strength of acid sites between them is similar. It is in good accordance with the results obtained by Martin Kubů *et al.*[17]

3.2 Acidity characterization

The NH_3-TPD curves of IM-5 and ZSM-5 (Z-110) are shown in Fig. 4. The spectrum of all samples can be divided into two different NH_3 desorption peaks at low and high temperatures, corresponding to weak and strong acid sites, respectively. Both the low and high temperature peaks shift to lower temperature with the increase of SiO_2/Al_2O_3. The results demonstrate that the H_2SiF_6 treatment reduced both weak and strong acid strength of IM-5.

The amount of acid obtained from NH_3-TPD profiles are summarized in Table 2. It is clear that H_2SiF_6 treatment has a significant effect on the acid amount of IM-5 sample. Both the strong and the weak acid decrease with the increase of H_2SiF_6 concentration. The concentrations of the weak acid sites decreased to a larger extent. It is generally accepted that the strong acid sites enhance the side reactions such as EB isomerization and cracking, leading to the formation of xylene and coke. Hence, the decreased concentration of strong acid sites in H_2SiF_6 treated IM-5 samples is expected to improve the catalytic performance in the alkylation of benzene with ethylene reaction. The acid concentration between I-110 and Z-110 is comparable. The acidity of IM-5 and ZSM-5 was also investigated using FTIR spectroscopy with pyridine as a probe molecule. The results obtained according to the corresponding extinction coefficient of Brønsted and Lewis acid sites are listed in Table 2. It was reported that the aqueous fluorosilicate treatment led to the substitution of an Al atom by an Si atom in the zeolite framework, leading to a sharp decrease in the concentration of Brønsted acid sites ascribed to the extraction of framework Al atom.[33] As shown in Table 2, both the Brønsted and Lewis acid concentration dropped with the increase of H_2SiF_6 concentration. The B/L ratio increased in the lower

Table 2 The acidity properties of IM-5 and ZSM-5 samples

		473 K			623 K		
Sample	mmol NH_3 per g	Brønsted acid (μmol g^{-1})	Lewis acid (μmol g^{-1})	B/L	Brønsted acid (μmol g^{-1})	Lewis acid (μmol g^{-1})	B/L
I-40	1.30	180.0	51.4	3.5	94.4	36.5	2.6
I-80	0.82	114.2	31.7	3.6	88.8	31.7	2.8
I-110	0.66	85.2	23.0	3.7	79.7	24.2	3.3
I-140	0.58	63.1	22.3	2.8	48.6	23.3	2.1
I-170	0.28	33.2	13.4	2.5	22.4	12.6	1.8
Z-110	0.69	86.1	26.2	3.3	80.2	23.6	3.4

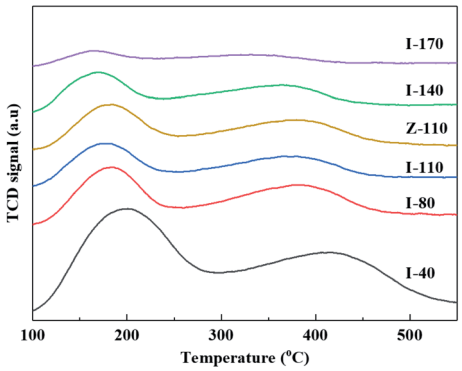

Fig. 5 NH_3-TPD curves of IM-5 and ZSM-5 samples.

degree of dealumination. However, the values declined considerably at a higher degree of extraction of Al atom. It is common knowledge that the production of a Brønsted acid site originated from the substitution of a Si atom by an Al atom in the framework of zeolite,[34] while the Lewis acid site is a coordinative unsaturated Al^{3+}. Thus, the coordinative of Al atom in zeolite framework varied with the increase of H_2SiF_6 concentration, which was consistent with the ^{27}Al NMR results. In short, increasing H_2SiF_6 concentration caused the total acid sites to decrease. Furthermore, there were no obvious difference in the total acid sites and B/L ratio of I-110 and Z-110 samples (Fig. 5 and Table 2).

3.3 Catalytic performance in benzene alkylation with ethylene

3.3.1 Effect of reaction temperature. This section investigates the ethylene conversion, EB and EB + DEB selectivity and xylene content of IM-5(I-40) as a function of reaction temperature to prove the feasibility of using IM-5 zeolite as a catalyst in benzene alkylation with ethylene reaction at a relative low temperature. It can be seen from Fig. 6(a) that the ethylene

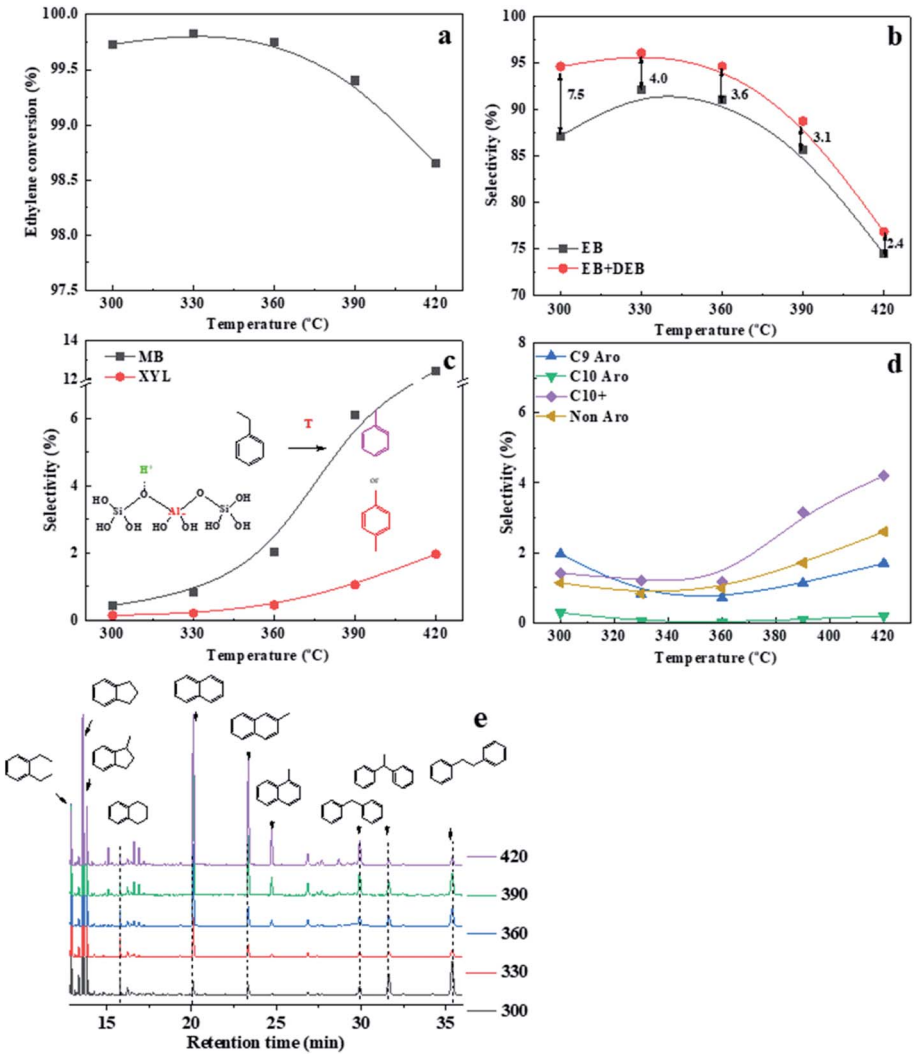

Fig. 6 The effect of reaction temperature on ethylene conversion (a), EB and EB + DEB selectivity (b), toluene (MB) and xylene (c) selectivity, by-products selectivity (d) as well as GC-MS total ion chromatogram of the heavier product (e). (The structures annotated above the chromatogram are peak identifications made by comparing the mass spectra with those in the NIST database). Reaction conditions: pressure = 0.8 MPa, WHSV = 0.5 h^{-1}, benzene/ethylene = 8.5 mol mol^{-1}.

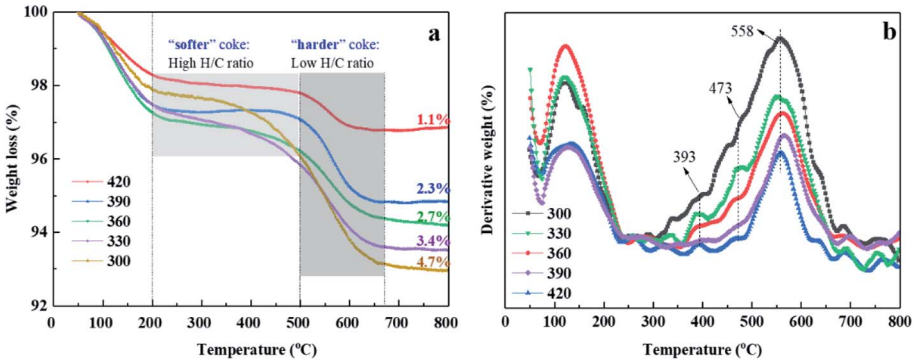

Fig. 7 TGA (a) and DTG (b) curves of the used samples after 12 h on stream.

conversion is always higher than 98.5% at all reaction temperatures. Moreover, the ethylene conversion decreases slightly with the reaction temperature due to the dealkylation reaction at a higher temperature.[35] Both the EB and (EB + DEB) selectivity are enhanced with the decreasing temperature, reaching a highest value at 330 °C (Fig. 6(b)). While the by-products selectivity, such as C_9 aromatics (*n*- and iso-propyl, methyl-ethylbenzene), C_{10} aromatics (butylbenzene), and heavier products deceased greatly (Fig. 6(d)) as the cracking and alkyl transfer reaction is deeply inhibited.[36] If the reaction temperature drops further, both the selectivity to EB and (EB + DEB) will decrease due to the oligomerization of ethylene and the subsequent alkylation reaction at lower temperatures.[37,38] The formation of bulky products such as diphenyl methane and diphenyl-ethane are accelerated in low reaction temperatures (Fig. 6(e)). It is hard for bulky products to diffuse out of the zeolite channel, and subsequently block the zeolite pore channels. Consequently, the activity and stability of the catalyst are reduced.[39–42] This can also be further evidenced through the TGA and DTG analysis of the used zeolites. Fig. 7(a) shows that all TGA curves display two main weight loss events. The first weight loss event before ~200 °C is mostly due to desorption of water and/or light aromatics adsorbed in the spent catalysts. However, the second weight loss event at higher temperatures (above 200 °C) is more complex. The complexity can be evidenced by the weight loss peaks at around 393 °C, 473 °C and 558 °C in Fig. 7(b), which belong to different coke species. When reaction occurred in 420 °C, the second weight loss event arises at significantly higher temperatures of 500–670 °C. This is associated with the oxidation of "harder" coke deposited on the catalyst during the alkylation reaction.[43] Moreover, the second weight loss event arises at a significantly lower and broader temperature range of 200–500 °C when the reaction temperature decreased. Such low and broad decomposition temperatures is likely due to the desorption or oxidation of "softer" coke (polymerization of ethylene). These polymerized olefins could be adsorbed strongly onto the acid sites of the zeolite,[44] thus inhibiting the benzene alkylation reaction and leading a lower EB and EB + DEB selectivity (*e.g.* 300 °C in Fig. 6(b)). However, the yielding of xylene and toluene, which are mainly originated from isomerization or cracking of EB, is significantly inhibited at low reaction temperatures (Fig. 6(c)). Reducing the xylene formation is gaining more and more attentions as it is one of the most important aims for the practical use of catalyst. The optimum reaction temperature of IM-5 is 330 °C in the gas phase alkylation of benzene with ethylene. A detailed reaction network was proposed based on the product distribution, a (Scheme 1).

3.3.2 Effect of Si/Al_2 ratio. Apart from decreasing the xylene yield, the other aim of benzene alkylation with ethylene is to increase the ethyl (EB + DEB) yield. The goal can be achieved by adjusting the acidity of the zeolite.[5,45] Fig. 8 shows the catalytic performance of the IM-5 with different Si/Al_2 ratios in benzene alkylation with ethylene. It can be seen that the increase of Si/Al_2 ratio from 40 to 110 did not have a significant effect on the

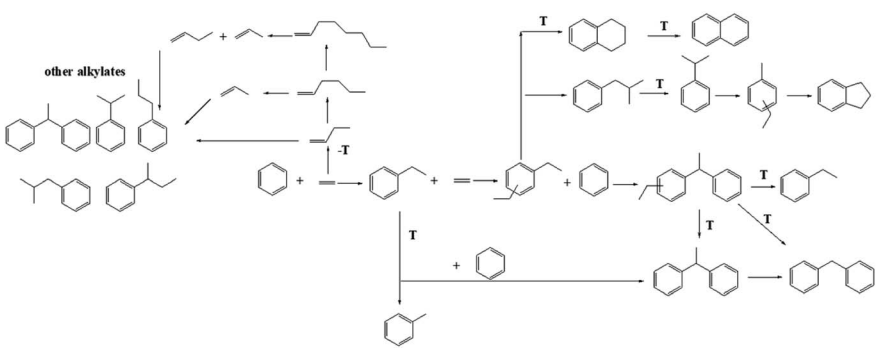

Scheme 1 Reaction network of benzene alkylation with ethylene *T*: reactions kinetically favored at higher temperatures. −*T*: reactions kinetically favored at lower temperatures.

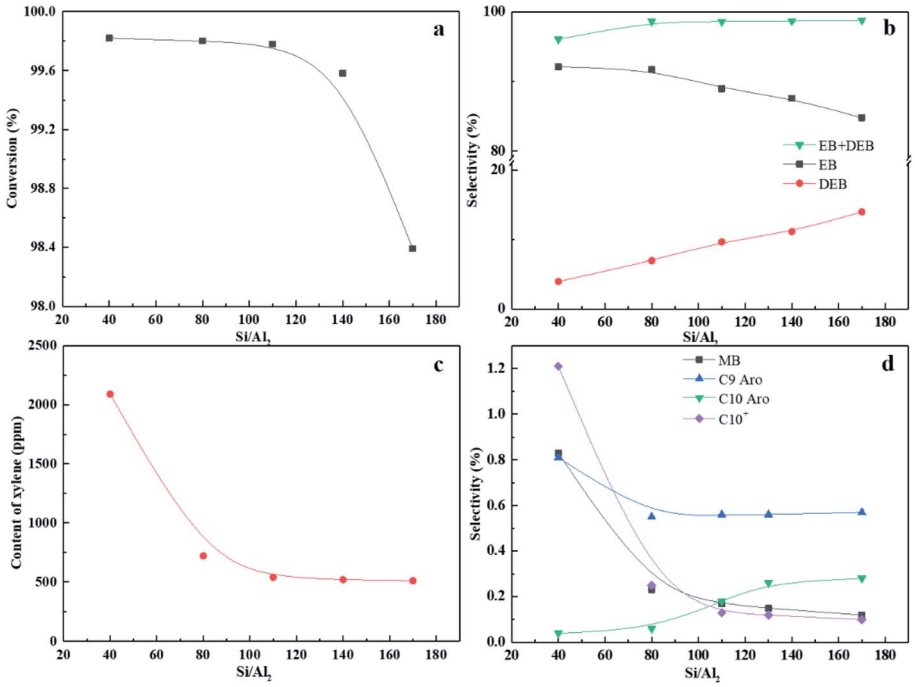

Fig. 8 The influence of Si/Al_2 ratio on ethylene conversion (a), EB, EB + DEB selectivity (b), content of xylenes (c) and by-products selectivity (d). Temperature = 330 °C, pressure = 0.8 MPa, WHSV = 0.5 h^{-1}, benzene/ethylene = 8.5 : 1 mol mol^{-1}.

conversion of ethylene (Fig. 8(a)), with a slight decrease from 99.82% to 99.78%. However, there was a visible rise in EB + DEB selectivity (Fig. 8(b)) from 96.06% to 98.60%. Especially, the xylene content decreased from 2089 to 539 ppm, indicating that the zeolite with a Si/Al_2 ratio of 110 can effectively suppress the formation of side products. This is mainly due to the decrease in density and strength of Brønsted acid sites of IM-5 during the H_2SiF_6 treatment,[46] which suppressed the ethylene oligomerization and coke formation.[47,48] This can also be explained with the significant increase of mesopore volume of I-110. With a shorter diffusion path length, the product is more likely to transport out of the zeolite channel, decreasing the further alkylation or oligomerization reaction.[7]

The zeolite activity declined from 99.78% to 98.39%, while the EB + DEB selectivity and xylene content kept almost remained almost unchanged after the Si/Al_2 ratio was increased to 170. Thus, 110 was considered as the optimum Si/Al_2 ratio for IM-5 in catalyzing benzene alkylation with ethylene. It should be noted that DEB is an exceptive by-product, which is generated by consecutive alkylation of EB with ethylene and can be used to yield EB *via trans*-alkylation with benzene.[49] The DEB selectivity was enhanced with the increase of Si/Al_2 ratio and the EB selectivity decreased as a result. This is due to the higher intrinsic reactivity of ethylbenzene compared with benzene. It is reported that the reactivity of alkyl benzene molecules increases with increasing number of alkyl groups on the benzene ring.[50] Thus, the subsequent alkylation of EB with ethylene to DEB was accelerated at IM-5 with a lower amount of Brønsted acid sites.

Fig. 9 shows the TGA and DTG curves of the used catalysts after 12 h on stream. With an increase in the Si/Al_2 ratio, the second weight loss of the IM-5 showed a more uniform loss rate. The result suggests that the weight loss is not associated with the formation of harder coke, but likely due to the desorption or oxidation of polymerization of ethylene.[51] The amount of coke deposits was calculated in the temperature range of 200 °C to 700 °C. Obviously, the coke amount formed on the IM-5 zeolite is decreased owing to the reducing of amount and strength of

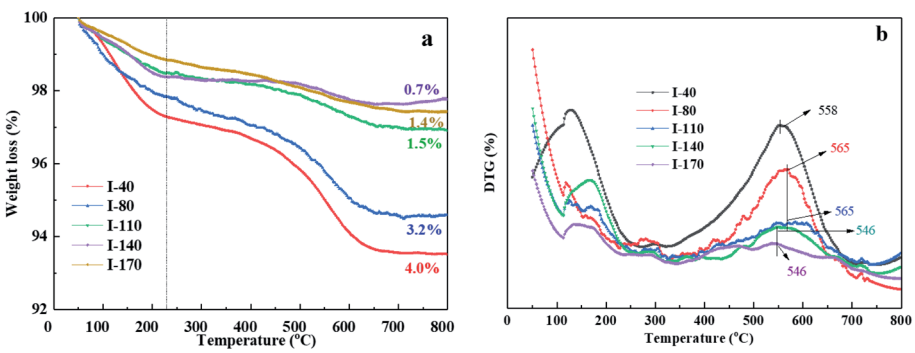

Fig. 9 TGA (a) and DTG (b) curves of the used samples with different Si/Al_2 ratio after 12 h on stream.

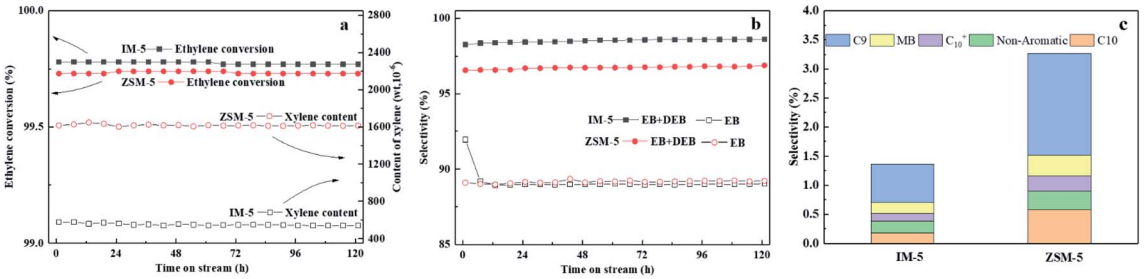

Fig. 10 Ethylene conversion and xylene content *versus* time on stream (a), selectivity (b) and by-products selectivity (c) in 120 hour-lifetime test on the IM-5 and the ZSM-5 samples. Reaction conditions: temperature = 330 °C, pressure = 0.8 MPa, WHSV = 0.5 h^{-1}, benzene/ethylene = 8.5 : 1 mol mol^{-1}.

acid sites at first. However, I-170 sample exhibits a similar coke amount with that of I-110. This may be because the low amount of acid sites is insufficient to alkylate the benzene with ethylene. The ethylene react with each other to form ethylene oligomerization. This is also evident with the incomplete ethylene conversion (Fig. 8(a)) and higher butyl selectivity (Fig. 8(d)). In addition, it was found that there was a good correspondence between the HF factor and the carbon deposition rate over IM-5 samples. As shown in Fig. S1,† on the whole, the carbon deposition rate decreases with the increase of HF (×100). Apart from the first peak corresponding to the physical adsorption of water/light aromatics, it can be seen from the DTG curves shown in Fig. 9(b) that another two weight loss peaks are observed at 420 °C and 560 °C, which belong to the different coke species formed on various acid sites with different strengths. Moreover, the decomposition peaks shift to lower temperature at both high and low amount of acid sites, indicating that the coke species were easier to eliminate.

3.3.3 Comparison of IM-5 and ZSM-5. In order to evaluate the stability of IM-5 120 hour-lifetime tests were carried out. ZSM-5 with a similar acid property was comparatively investigated to clarify the effect of zeolite topology on catalytic performance in vapor-phase alkylation of benzene with ethylene. In this section, the reaction temperature was 330 °C which was optimized in Section 3.3.1. Fig. 10(a) shows the ethylene conversion and xylene content of IM-5(I-110) and ZSM-5(Z-110). The ethylene conversion of both samples is nearly complete after 120 h on stream no obvious deactivation is found during the period of reaction. Compared with ZSM-5, a slightly higher ethylene conversion is found on IM-5. To further clarify the effect of pore topology on catalytic performance in benzene alkylation with ethylene, the detailed product distributions of IM-5 and ZSM-5 are given in Fig. 10(b) and (c).

The main products of IM-5 and ZSM-5 were ethylbenzene and di-ethylbenzene. IM-5 and ZSM-5 showed a similar ethylbenzene selectivity. However, the EB + DEB selectivity (98.4%) for IM-5 is higher that of ZSM-5 (96.6%). The higher DEB selectivity on IM-5 contributed to this increase. Considering the two samples have a similar amount of acid sites as well as B/L ratio, we speculate that the pore structure of IM-5 (pore diameter: 5.4–5.9 Å) is more conductive to the formation and diffusion of DEB (d: *m*-DEB ≈ 5.5 Å nm, *p*-DEB ≈ 4.3 Å and *o*-DEB ≈ 7.8 Å) than ZSM-5 (pore diameter: 5.3–5.6 Å). Compared to ZSM-5 the diffusion properties of aromatics, such as toluene and *m*-xylene, in IM-5 proved to be better in the adsorption experiment.[20,21]

In addition, there was a large difference in xylene content between IM-5 and ZSM-5. The xylene content is at about 1600 ppm on ZSM-5 compared to 540 ppm on IM-5. The difference can be attributed to the different pore structures of IM-5 and ZSM-5. In terms of reducing of xylene yield, IM-5 zeolite exhibited a better catalytic performance than ZSM-5 in practical use.

C_9 and C10 aromatics were the major by-products for both IM-5 and ZSM-5 samples (Fig. 9(c)). Notably, the selectivity of C_9 and C_{10} aromatics on ZSM-5 was higher than IM-5. In the alkylation of benzene with ethylene reaction, the active ethylene species formed on a Brønsted acid site of 10-ring member zeolite can follow two major routes: (1) it can alkylate with benzene to produce EB which can later undergo subsequent reactions to produce mainly di-ethylbenzene. (2) It can react with another one or more ethylene molecules to produce a C_4,

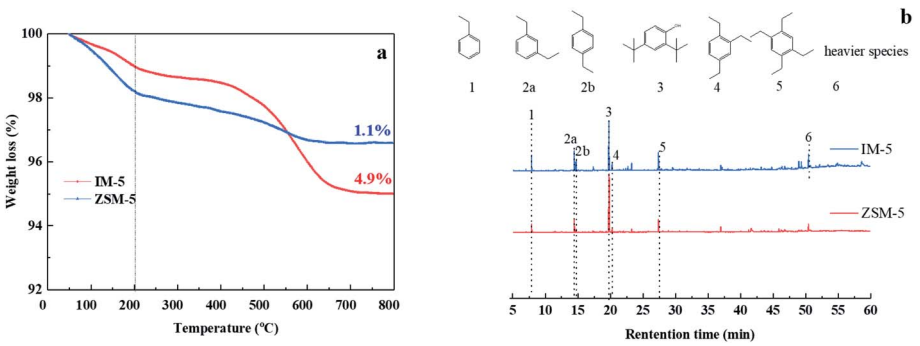

Fig. 11 TGA curves (a) and GC-MS analysis of retained species (b) of the reacted IM-5 and ZSM-5 samples after 120 hour-lifetime test.

C_6 species which can further transform *via* alkylation, oligomerization, isomerization or cracking yielding other alkylbenzenes and olefins (Scheme 1).[49] Compared to the free diameter (8.6 Å) at the channel intersection in ZSM-5, a large channel intersection (10.4 Å) was formed due to much more complex channel intersections.[52] This distinctive pore structure enables IM-5 to accommodate bulky intermediates in catalytic reactions. Thus, the di-ethylbenzene was much easier to form and to diffuse out of the channel system, leading to a higher DEB selectivity. Babatunde Ogunbadejo *et al.*[53] has also found that IM-5 had a higher DEB selectivity compared to ZSM-5 during toluene alkylation with ethanol reaction due to the larger internal reaction volume of IM-5. In contrast, the diffusion rate of DEB in ZSM-5 is much slower, while the ethylene oligomerization-cracking and subsequent alkylation with benzene is accelerated, leading to a much higher C_9 and C_{10} aromatics selectivity.

Fig. 11(a) shows the TGA curves of used IM-5 and ZSM-5 after 120 hours reaction. IM-5 has a higher coking amount (4.9%) than that of ZSM-5 (1.1%). Fig. 11(b) shows that both of the reacted IM-5 and ZSM-5 contained substantial amounts of ethyl-substituted benzenes with 1 to 4 ethyl groups. There is a lower proportion of ethyl-substituted benzenes but a higher proportion of heavier species (6) on IM-5 compared to ZSM-5. This is further evidence that IM-5 possesses a better diffusion property for di-ethylbenzene due to its larger pores size.

4. Conclusion

The reaction temperature has an important effect on the catalytic performance of IM-5 in vapor phase benzene alkylation with ethylene. It is found that both the highest ethylene conversion and EB + DEB selectivity were obtained at a reaction temperature of 330 °C over IM-5. The xylene yield is inhibited greatly with reducing of the reaction temperature. The H_2SiF_6 treatment could effectively decrease the total amount and strength of acid sites of IM-5 without destroying its framework. The selectivity to EB + DEB improved while the formation of xylene was inhibited and the coke amounts decreased over modified IM-5 due to the decline in acid amount and acid strength. Compared with ZSM-5 ($Si/Al_2 = 110$), the unique pore system with larger channel crossing volume and bigger pore mouth gives IM-5 better diffusion properties, leading to superior activity, equivalent stability, similar EB selectivity, higher DEB selectivity as well as lower C_9–C_{10} aromatics and xylene selectivity. In conclusion, IM-5 is a promising catalytic material for vapor-phase alkylation of benzene with ethylene.

Conflicts of interest

There are no conflicts to declare.

Acknowledgements

The author(s) would like to thank the Department of Analysis at Sinopec in Research Institute of Petroleum Processing for its support.

References

1 T. F. Degnan, C. M. Smith and C. R. Venkat, *Appl. Catal., A*, 2001, **221**, 283–294.
2 C. Perego and P. Ingallina, *Catal. Today*, 2002, **73**, 3–22.
3 W. Yang, Z. Wang, H. Sun and B. Zhang, *Chin. J. Catal.*, 2016, **37**, 16–26.
4 Dilute ethylene alkylation with ethylene, WO2013006603A2, 2013.
5 L. Zhang, Z. Wang, H. Sun and W. Yang, *Ind. Catal.*, 2016, **24**, 1–7.
6 X. X. Zhu, F. C. Chen, J. An, P. Zeng and L. Y. Xu, *Adv. Mater. Res.*, 2011, **233–235**, 1708–1713.
7 C. H. Christensen, K. Johannsen, I. Schmidt and C. H. Christensen, *J. Am. Chem. Soc.*, 2003, **125**, 13370–13371.
8 Z. Shen, C. Ma, J. He, D. Wang, H. Sun, Z. Zhu and W. Yang, *Appl. Catal., A*, 2019, **577**, 20–27.
9 P. G. Smirniotis and E. Ruckenstein, *Ind. Eng. Chem. Res.*, 1995, **34**, 1517–1528.
10 M. Lu, Y. Guo, Z. Zhu, W. Yang and W. Lu, *Petrochem. Technol.*, 2001, **30**, 270–274.
11 S. Liu, F. Chen, S. Xie, P. Zeng, X. Du and L. Xu, *J. Nat. Gas Chem.*, 2009, **18**, 21–24.
12 S. Al-Khattaf, C. D'Agostino, M. N. Akhtar, N. Al-Yassir, N. Y. Tan and L. F. Gladden, *Catal. Sci. Technol.*, 2014, **4**, 1017–1027.
13 K. Gołąbek, K. A. Tarach, U. Filek and K. Góra-Marek, *Spectrochim. Acta, Part A*, 2018, **192**, 464–472.
14 IM-5 zeolite, A process for its preparation and catalytic applications thereof, US6136290, 2000.
15 C. Baerlocher, F. Gramm, L. Massüger, L. B. McCusker, Z. He, S. Hovmöller and X. Zou, *Science*, 2007, **315**, 1113–1116.
16 H.-K. Min, S. H. Cha and S. B. Hong, *ACS Catal.*, 2012, **2**, 971–981.
17 M. Kubů, S. I. Zones and J. Čejka, *Top. Catal.*, 2010, **53**, 1330–1339.
18 A. Corma, J. Mengual and P. J. Miguel, *Appl. Catal., A*, 2013, **460–461**, 106–115.
19 A. Corma, J. Martínez-Triguero, S. Valencia, E. Benazzi and S. Lacombe, *J. Catal.*, 2002, **206**, 125–133.
20 A. Corma, A. Chica, J. M. Guil, F. J. Llopis, G. Mabilon, J. A. Perdigón-Melón and S. Valencia, *J. Catal.*, 2000, **189**, 382–394.
21 Q. Yu, Z. Huang, H. Sun, L. Li, X. Zhu, S. Ren and B. Shen, *Ind. Eng. Chem. Res.*, 2018, **57**, 14448–14459.
22 Q. Chen, Y. Wang, S. Min, M. Xuhong and S. Xingtian, *Acta Pet. Sin.*, 2010, **26**, 165–170.
23 J. Chen, C. Zhang, Y. Wang, M. Sun, X. Mu and X. Shu, *Acta Pet. Sin.*, 2013, **29**, 757–765.
24 M. Kubů, N. Žilková, S. I. Zones, C.-Y. Chen, S. Al-Khattaf and J. Čejka, *Catal. Today*, 2015, **259**, 97–106.
25 C. Yang, S. Xie, H. Liu, W. Xin, C. Feng, X. Li, S. Liu, L. Xu and P. Zeng, *Catal. Lett.*, 2018, **148**, 2030–2041.
26 X. Meng, D. Yi, L. Shi and N. Liu, *Pet. Sci. Technol.*, 2020, **38**, 501–508.
27 S. Lee, *J. Catal.*, 2003, **215**, 151–170.

28 H. Najar, M. S. Zina and A. Ghorbel, *React. Kinet. Mech. Catal.*, 2010, **100**, 385–398.
29 S. H. Lee, D. K. Lee, C. H. Shin, Y. K. Park, P. A. Wright, W. M. Lee and S. B. Hong, *J. Catal.*, 2003, **215**, 151–170.
30 K. Egeblad, C. H. Christensen, M. Kustova and C. H. Christensen, *Chem. Mater.*, 2008, **20**, 946–960.
31 E. Xing, Y. Shi, W. Xie, F. Zhang, X. Mu and X. Shu, *Microporous Mesoporous Mater.*, 2016, **236**, 54–62.
32 J. Pérez-Ramírez, C. H. Christensen, K. Egeblad, C. H. Christensen and J. C. Groen, *Chem. Soc. Rev.*, 2008, **37**, 2530–2542.
33 Y. He, C. Li and E. Min, *Stud. Surf. Sci. Catal.*, 1989, **49**, 189–197.
34 J. Van der Mynsbrugge, A. Janda, L.-C. Lin, V. Van Speybroeck, M. Head-Gordon and A. T. Bell, *ChemPhysChem*, 2018, **19**, 341–358.
35 J. Das, Y. S. Bhat and A. B. Halgeri, *Ind. Eng. Chem. Res.*, 1993, **32**, 2525–2529.
36 J. M. Serra, E. Guillon and A. Corma, A rational design of alkyl-aromatics dealkylation–transalkylation catalysts using C8 and C9 alkyl-aromatics as reactants, *J. Catal.*, 2004, **227**, 459–469.
37 S. Siffert, L. Gaillard and B. L. Su, *J. Mol. Catal. A: Chem.*, 2000, **153**, 267–279.
38 K. Becker, *J. Catal.*, 1973, **28**, 403–413.
39 G. Mirth, J. Cejka, J. Krtil and J. A. Lercher, *Stud. Surf. Sci. Catal.*, 1994, **88**, 241–248.
40 P. B. Venuto, L. A. Hamilton and P. S. Landis, *J. Catal.*, 1966, **5**, 484–493.
41 J. Čejka, B. Wichterlová and S. Bednářová, *Appl. Catal., A*, 1991, **79**, 215–226.
42 T. Odedairo and S. Al-Khattaf, *Appl. Catal., A*, 2010, **385**, 31–45.
43 K. Bian, A. Zhang, H. Yang, B. Fan, S. Xu, X. Guo and C. Song, *Ind. Eng. Chem. Res.*, 2020, **59**, 22413–22421.
44 E. G. Derouane, J.-P. Gilson and J. B. Nagy, *J. Mol. Catal.*, 1981, **10**, 331–340.
45 M. Osman, L. Atanda, M. M. Hossain and S. Al-Khattaf, *Chem. Eng. J.*, 2013, **222**, 498–511.
46 W. Xue Qin and W. Xiangsheng, *Acta Pet. Sin.*, 1994, **10**, 44–48.
47 L. Hexuan, Z. Yaru, T. Keyi and Z. Yingxian, *Chem. J. Chin. Univ.*, 1985, **6**, 191–196.
48 Y. Weimin, S. Hongmin and C. Qingling, *Adv. Fine Petrochem.*, 2002, **3**, 12–14.
49 C. Perego and P. Ingallina, *Green Chem.*, 2004, **6**, 274–279.
50 S. Al-Khattaf, M. N. Akhtar, T. Odedairo, A. Aitani, N. M. Tukur, M. Kubů, Z. Musilová-Pavlačková and J. Čejka, *Appl. Catal., A*, 2011, **394**, 176–190.
51 Y. Du and J. Ru, *Pet. Process. Petrochem.*, 2006, **37**, 31–36.
52 H.-K. Min and S. B. Hong, *J. Phys. Chem. C*, 2011, **115**, 16124–16133.
53 B. Ogunbadejo, A. Aitani, J. Čejka, M. Kubů and S. Al-Khattaf, *Chem. Eng. J.*, 2016, **306**, 1071–1080.